Influences of different factors on the three-dimensional heat transfer of spiral-coil energy pile group with seepage

Tian You and Hongxing Yang*

Renewable Energy Research Group, Department of Building Services Engineering, The Hong Kong Polytechnic University, Yucai Road, Hung Hom, Kowloon, Hong Kong, China

Abstract

Energy pile group is an important component of ground source heat pumps with foundation piles as ground heat exchangers. Among different energy piles, those with spiral pipes have a large heat exchange area between the pipe and the concrete, achieving good heat exchanging performance and wide applications. To analyze the influence of geometrical parameters (pile layout, pile spacing and pile depth) and external parameter (groundwater velocity) on the heat transfer of spiral-coil energy pile groups, a three-dimensional analytical model of spiral-coil energy pile groups with seepage is used, considering the thermal interaction among different piles, the geometry of spiral pipe and the velocity of groundwater. The soil temperature distribution in the energy pile group is studied under conditions with different factors (pile layouts: 3×2, L shape and line shape; pile spacing distances: 3, 5 and 7 m; pile depths: 10, 30 and 50 m; and groundwater velocities: 0, 1.2×10^{-6} and 2.0×10^{-6} m/s). The 3-year outlet fluid temperature of energy pile group affected by the above different factors under different inlet fluid temperatures and velocities or soil thermal exchange ratios is investigated. Results show that for the low fluid velocity inside the piles, the influence of above factors on the thermal performance of energy piles is more obvious. Large groundwater velocity, line shape pile layout, large pile spacing distance and short pile depth can alleviate the long-term temperature variation caused by unbalanced soil heat exchange. This work will facilitate the research, design and application of the energy pile group in ground source heat pumps.

Keywords: energy pile group; influential factors; analytical model; soil temperature distribution; seepage

1. INTRODUCTION

Ground source heat pump is an efficient and clean air conditioning technology, having a rapid increasing potential in application [1, 2]. Ground heat exchangers [3, 4], such as boreholes and energy piles, are important components to affect the performance of soil heat exchange and the whole system [5, 6]. Energy piles [7, 8], with burying pipes inside the concrete to fully use the pile structures of buildings, can reduce the drilling cost and the occupied land compared with boreholes [9]. Among different buried pipes (U pipe [10, 11], W pipe [12] or spiral pipe [13, 14]), the energy piles with spiral pipes have the largest heat exchanging area between the pipe and the concrete, achieving better thermal performance and wider practical applications [15].

Since the thermal performance of ground heat exchangers directly affects the system performance of ground source heat pumps (GSHPs), many researchers conducted studies on the model development [16, 17] and influential factors analysis of ground heat exchangers [18]. Zhang *et al.* [19] developed the analytical model of a single energy pile considering the practical geometry of the spiral coil and the groundwater seepage. Cimmino *et al.* [20] proposed the model of a boreholes group considering the thermal interaction among different boreholes in a group. Choi *et al.* [21] conducted two-dimensional numerical simulations of an energy piles group while it ignored the pipe geometry and the pile depth. Little research is conducted on three-dimensional thermal analysis of the energy piles group, considering the thermal interactions among piles, the geometry of the spiral pipe and the velocity of groundwater.

Zhao *et al.* [22] investigated the influence of spiral pitch on the thermal behaviors of energy piles with spiral tube heat exchanger and found out the thermal resistances and heat transfer rates of energy piles with four kinds of spiral pitches. Zhang *et al.* [23] and You *et al.* [24] analyzed the influence of groundwater seepage on the performance of GSHP with an energy pile. The groundwater can indeed improve the system performance and its influential roles are different under the conditions with different underground mediums, types of refrigerant, the directions of groundwater velocity and the temperatures of chilled water. Yoon *et al.* [25] and Zhao *et al.* [26] studied the thermal performance of energy piles with different types of heat exchanging pipes including U-shaped, W-shaped and spiral-shaped pipes. The spiral pipe is estimated to have the best thermal performance among these three different types of pipes. Yang *et al.* [27] tested the thermal performance of a spiral coil energy pile affected by the different types of pile mediums with different thermal diffusivities and the intermittent operation control mode. For the energy pile group, group parameters such as the pile layout, pile spacing, pile depth and surrounding groundwater velocity are significant to the thermal performances of energy piles and the system. However, the studies on these above factors are not enough.

In this paper, a three-dimensional analytical model of spiral energy pile group with seepage will be established based on the superposition principle. The investigated different influential factors in the energy pile group will include the pile layout, pile spacing, pile depth and groundwater velocity. The soil temperature distribution in the energy pile group will be studied under the conditions with the above different factors. The 3-year outlet fluid temperature of the energy pile group will be investigated with the influence of the above different factors under different inlet fluid temperatures and velocities and under different soil heat exchange ratios. Towards these ends, the investigated thermal characteristics of an energy piles group will guide the design and application of energy piles.

2. ENERGY PILE GROUP MODEL WITH SEEPAGE

The schematic diagram of the energy piles group is shown in Figure 1. The spiral pipes are buried in the pile foundations of a building to compose the energy piles and to exchange heat with the ground. The thermal interaction among different piles, the geometry of the spiral pipe and the groundwater seepage affect the heat transfer of the energy piles group. In this paper, the three-dimensional energy pile group model with seepage which is based on the analytical model of single spiral coil energy pile and the superposition principle is adopted to analyze the heat transfer of energy piles group by considering the above factors.

2.1. Different heat fluxes of energy piles
The heat flux matrix is shown in Equation (1). Since the heat fluxes of energy piles interact each other, they should be calculated
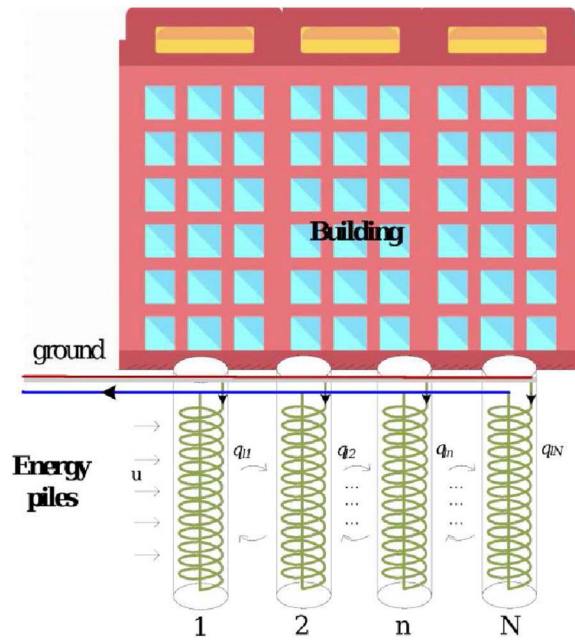

Figure 1. *Schematic diagram of the energy piles group with seepage.*

Figure 2. *Sandbox experiment [8].*

simultaneously by the matrix. The detailed derivation of the heat flux matrix is illustrated in our previous study [8]. Not only does the Equation (1) calculate the heat fluxes of different piles in a coupled way, but also it combines the inside and outside heat transfers of the spiral pipe in each energy pile. The heat transfer inside the pipe is equal to the internal energy difference between inlet and outlet fluid. The heat transfer across the pipe wall is based on the equivalent thermal resistance between the fluid and the outer pipe wall. The heat transfer outside the pipe is calculated by the seepage model of a single spiral-coil energy pile (Equation (2)).

$$\left[q_{l,1}(j\Delta\tau) \; q_{l,2}(j\Delta\tau) \; \ldots \; q_{l,n}(j\Delta\tau) \; \ldots \; q_{l,N}(j\Delta\tau) \right]^T = A^{-1} \times B \tag{1}$$

$$A = \begin{bmatrix} \frac{R_p \times H}{L_{pipe}} + \frac{H}{2c_f m_f} + \frac{\Theta_{1,1}(\Delta\tau)}{\lambda_s} & \frac{\Theta_{2,1}(\Delta\tau)}{\lambda_s} & \cdots & \frac{\Theta_{n,1}(\Delta\tau)}{\lambda_s} & \cdots & \frac{\Theta_{N,1}(\Delta\tau)}{\lambda_s} \\ \frac{\Theta_{1,2}(\Delta\tau)}{\lambda_s} & \frac{R_p \times H}{L_{pipe}} + \frac{H}{2c_f m_f} + \frac{\Theta_{2,2}(\Delta\tau)}{\lambda_s} & \cdots & \frac{\Theta_{n,2}(\Delta\tau)}{\lambda_s} & \cdots & \frac{\Theta_{N,2}(\Delta\tau)}{\lambda_s} \\ \cdots & \cdots & & \cdots & & \cdots \\ \frac{\Theta_{1,n}(\Delta\tau)}{\lambda_s} & \frac{\Theta_{2,n}(\Delta\tau)}{\lambda_s} & \cdots & \frac{R_p \times H}{L_{pipe}} + \frac{H}{2c_f m_f} + \frac{\Theta_{n,n}(\Delta\tau)}{\lambda_s} & \cdots & \frac{\Theta_{N,n}(\Delta\tau)}{\lambda_s} \\ \cdots & \cdots & & \cdots & & \cdots \\ \frac{\Theta_{1,N}(\Delta\tau)}{\lambda_s} & \frac{\Theta_{2,N}(\Delta\tau)}{\lambda_s} & \cdots & \frac{\Theta_{n,N}(\Delta\tau)}{\lambda_s} & \cdots & \frac{R_p \times H}{L_{pipe}} + \frac{H}{2c_f m_f} + \frac{\Theta_{N,N}(\Delta\tau)}{\lambda_s} \end{bmatrix}$$

(1a)

$$B = \begin{bmatrix} T_{in}(j\Delta\tau) - t_0 + \sum_{ni=1}^{N} \left\{ q_{l,ni}((j-1)\Delta\tau) \times \Theta_{ni,1}(\Delta\tau) - \sum_{i=2}^{j-1}[q_{l,ni}(i\Delta\tau) - q_{l,ni}((i-1)\Delta\tau)] \times \Theta_{ni,1}((j-i+1)\Delta\tau) - q_{l,ni}(\Delta\tau) \times \Theta_{ni,1}(j\Delta\tau) \right\} / \lambda_s \\ T_{in}(j\Delta\tau) - t_0 + \sum_{ni=1}^{N} \left\{ q_{l,ni}((j-1)\Delta\tau) \times \Theta_{ni,2}(\Delta\tau) - \sum_{i=2}^{j-1}[q_{l,ni}(i\Delta\tau) - q_{l,ni}((i-1)\Delta\tau)] \times \Theta_{ni,2}((j-i+1)\Delta\tau) - q_{l,ni}(\Delta\tau) \times \Theta_{ni,2}(j\Delta\tau) \right\} / \lambda_s \\ \cdots \\ T_{in}(j\Delta\tau) - t_0 + \sum_{ni=1}^{N} \left\{ q_{l,ni}((j-1)\Delta\tau) \times \Theta_{ni,n}(\Delta\tau) - \sum_{i=2}^{j-1}[q_{l,ni}(i\Delta\tau) - q_{l,ni}((i-1)\Delta\tau)] \times \Theta_{ni,n}((j-i+1)\Delta\tau) - q_{l,ni}(\Delta\tau) \times \Theta_{ni,n}(j\Delta\tau) \right\} / \lambda_s \\ \cdots \\ T_{in}(j\Delta\tau) - t_0 + \sum_{ni=1}^{N} \left\{ q_{l,ni}((j-1)\Delta\tau) \times \Theta_{ni,N}(\Delta\tau) - \sum_{i=2}^{j-1}[q_{l,ni}(i\Delta\tau) - q_{l,ni}((i-1)\Delta\tau)] \times \Theta_{ni,N}((j-i+1)\Delta\tau) - q_{l,ni}(\Delta\tau) \times \Theta_{ni,N}(j\Delta\tau) \right\} / \lambda_s \end{bmatrix}$$

(1b)

where q_l is the heat flux of energy pile, W/m; $\Delta\tau$ is the length of a time step, s; Θ is the dimensionless excess wall temperature of the spiral pipe; T_{in} is the inlet fluid temperature of each energy pile, °C; t_0 is the initial soil temperature, °C; λ_s is the thermal conductivity of the soil, W/(m·K); R_p is the equivalent thermal resistance between the fluid and the outer pipe wall, (°C·m)/W; c_f is the specific heat of fluid, J/(kg·K); m_f is the mass flow rate of fluid, kg/s; subscript n is the nth energy pile, ($n = 1, 2, \ldots, N$).

In Equation (1), the dimensionless soil temperature of a single energy pile with seepage (Θ) is calculated by Equation (2) [19]. It is obtained by the integration of g-function with the spiral line and the duration of heat release. The dimensionless soil temperature Θ represents the relationship between the practical soil temperature difference and heat flux.

$$\Theta = \frac{B}{16\pi^{5/2}} \int_0^{Fo} \frac{1}{(Fo - Fo')^{3/2}} \int_{2\pi H_1/B}^{2\pi H_2/B}$$

$$\exp\left[-\frac{[X - \cos\varphi' - S(Fo - Fo')]^2 + (Y - \sin\varphi')^2}{4(Fo - Fo')}\right]$$

$$\times \left\{ \exp\left[-\frac{(Z - B\varphi'/2\pi)^2}{4(Fo - Fo')}\right] \right.$$

$$\left. - \exp\left[-\frac{(Z + B\varphi'/2\pi)^2}{4(Fo - Fo')}\right] \right\} d\varphi' dFo'$$

(2)

$$\Theta = \frac{\lambda_s \times \theta}{q_l} = \frac{\lambda_s \times (t - t_0)}{q_l}$$

(2a)

2.2. Dimensionless soil temperature distribution and outlet fluid temperature

According to the superposition principle [28], the dimensionless soil temperature distribution of an energy piles group (Θ_{soil}) can be calculated by Equation (3). It is the superposition of dimensionless soil temperature influenced by each energy pile ($\Theta_{ni,soil}$) which is calculated by Equation (2).

$$\Theta_{soil}(j\Delta\tau) = \sum_{ni=1}^{N} \Theta_{ni,soil}(j\Delta\tau)$$

(3)

After the heat flux of each energy pile is calculated from the heat flux matrix and the inlet fluid temperature is given, the outlet fluid temperature of each energy pile can be calculated by Equation (4).

$$T_{out,n}(j\Delta\tau) = T_{in}(j\Delta\tau) - \frac{q_{l,n}(j\Delta\tau) \times H}{c_f m_f}$$

(4)

where H is the length of energy pile, m; $T_{out,n}$ is the outlet fluid temperature of the nth energy pile, °C.

2.3. Model validation

The sandbox experiment of a ground heat exchanger group is set up to validate the model [8]. The sandbox has a size of 1 m × 1 m × 1 m and buried with five heat exchanging pipes. The water flows in parallel into five pipes from a water bath with the temperature and velocity controls. Four thermocouples are buried in the middle depth of the sandbox to measure the soil temperatures at four typical positions.
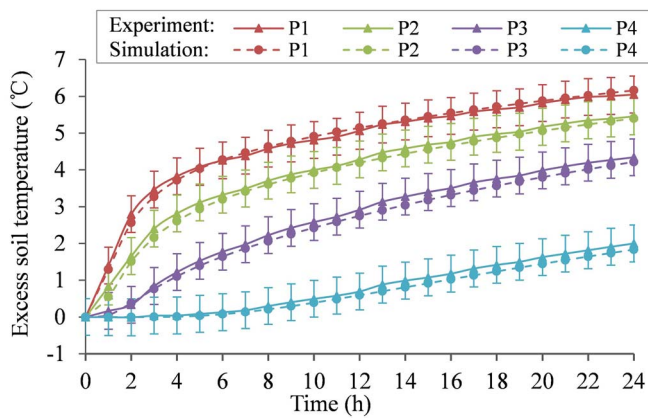
Figure 3. *Soil temperature comparison of experiment and simulation results [8].*

Keeping the excess temperature of pipe inlet at 10°C, the excess soil temperatures of four points are tested by the sandbox experiment and simulated by the above energy pile group model. The temperature comparison of experiment and simulation is shown in Figure 3. It is obvious that the temperature difference between these two methods is less than 0.25°C. The proposed three-dimensional energy pile group model has good accuracy.

3. RESULTS

Using the above model, the influence of the external parameter (the groundwater velocity) and the geometrical parameters (the pile layout, pile spacing distance and pile depth) of the energy pile group are illustrated. As shown in Table 1, the compared groundwater velocities are 0, 1.2×10^{-6} m/s and 2.0×10^{-6} m/s; pile layouts are matrix shape (3×2), L shape and line shape; pile spacing distances are 3, 5 and 7 m; pile depths are 10, 30 and 50 m. As a heating or cooling season is usually 4 months, the dimensionless soil temperature distribution after a 4-month operation is demonstrated for the cases with different influential factors. When the inlet fluid temperature and velocity are different, the 3-year outlet fluid temperature of energy piles affected by different factors are analyzed. For the energy pile group with different heat extractions and heat injections, the influence of different factors on the 3-year outlet fluid temperature of energy piles is investigated.

3.1. Dimensionless soil temperature distribution
The dimensionless soil temperature distributions after a 4-month operation influenced by different factors are investigated and illustrated in Figures 4–8.

3.1.1. *Groundwater velocity*
Keeping the pile depth at 50 m, pile spacing distance at 5 m and pile layout being 3×2, the dimensionless soil temperature distributions under different groundwater velocities (0 m/s,

Table 1. *Parameters of different studied cases with influential factors.*

Objective factor	Other factors
Groundwater velocities: $v = 0$, 1.2×10^{-6} m/s, and 2.0×10^{-6} m/s	Pile layout: matrix shape (3×2); Pile spacing distance: 5 m; Pile depth: 50 m
Pile layouts: matrix shape (3×2), L shape, and line shape	Groundwater velocity: 0; Pile spacing distance: 5 m; Pile depth: 50 m
Pile spacing distances: 3, 5 and 7 m	Groundwater velocity: 0; Pile layout: matrix shape (3×2); Pile depth: 50 m
Pile depths: 10, 30 and 50 m	Groundwater velocity: 0; Pile layout: matrix shape (3×2); Pile spacing distance: 5 m

1.2×10^{-6} m/s and 2.0×10^{-6} m/s) are shown in Figure 4. For the energy pile group without the seepage, the soil around the central energy pile has the highest temperature. The maximum dimensionless soil temperature is 0.77, and the minimum value is 0.07. Since the groundwater brings the released heat of the upstream energy piles along with the water flow, it reduces the temperature of the upstream soil. Compared to the upstream soil, the downstream soil has a higher temperature. When the groundwater velocity increases from 0 to 1.2×10^{-6} m/s and 2.0×10^{-6} m/s, the highest dimensionless soil temperature is reduced to 0.61 and 0.45, and the lowest dimensionless soil temperature is reduced to 0 in two cases.

3.1.2. *Group layouts*
The soil temperature distributions of the energy piles with different pile layouts, including 3×2 matrix shape, L shape and line shape, are shown in Figure 5. Compared to energy piles with 3×2 layout in Figure 5a, energy piles with L layout in Figure 5b and line layout in Figure 5c have much lower soil temperature due to the good condition of heat dispersion into the soil. The maximum dimensionless soil temperature is 0.65 in L layout and 0.61 in line layout. The minimum dimensionless soil temperature is 0.01 in L layout and 0.06 in line layout.
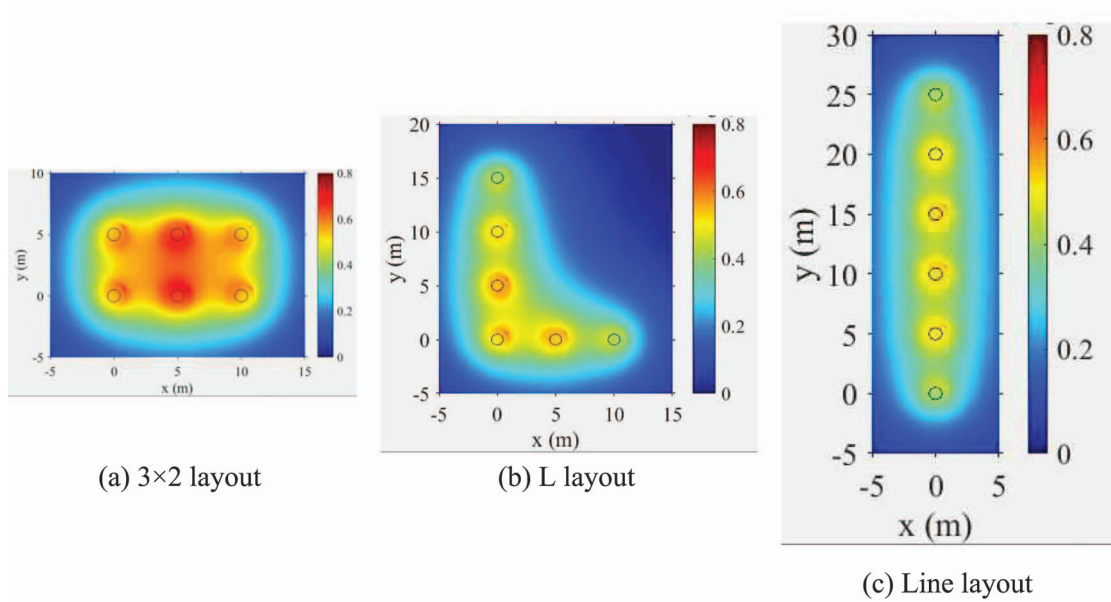
3.1.3. *Pile spacing distances*
The soil temperature distributions of the energy piles with different pile spacing distances (3, 5 and 7 m) are shown in Figure 6. The group with a 3-m pile spacing distance in Figure 6a has the highest soil temperature because less heat can be dispersed to the external soil due to the compact pile group. The maximum dimensionless soil temperature is 1.13 and the minimum value is 0.26. Large pile spacing distance can increase the occupied soil volume and enlarge the soil boundary, so the soil temperature is low in piles with 7 m spacing in Figure 6c. The maximum dimensionless soil temperature is 0.59, and the minimum value is 0.02.
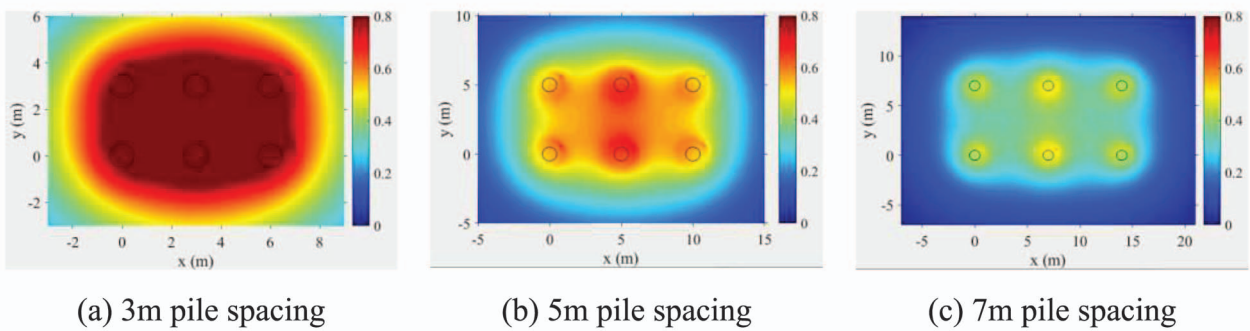
3.1.4. *Pile depths*
The dimensionless soil temperature distributions at the half depth of different energy piles are shown in Figure 7. Due to the heat
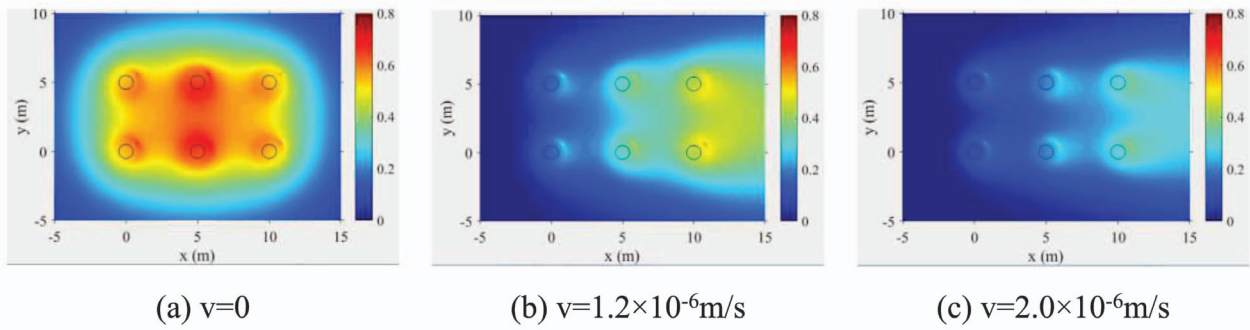
Figure 4. *Dimensionless soil temperature distribution influenced by different groundwater velocities (pile layout = 3 × 2, pile spacing distance = 5 m, pile depth = 50 m).*

Figure 5. *Dimensionless soil temperature distribution influenced by different pile layouts (v = 0, pile spacing distance = 5 m, pile depth = 50 m).*

Figure 6. *Dimensionless soil temperature distribution influenced by different pile spacing distances (v = 0, pile layout = 3 × 2, pile depth = 50 m).*

disperse from the soil surface, the pile group with a 10-m depth has the lowest soil temperature. The maximum dimensionless soil temperature is 0.75, and the minimum value is 0.06 of piles with 10 m depth in Figure 7a. With the depth increasing from 10 to 50 m, less percentage of heat is dispersed from the soil surface and the soil temperature is the highest for the case with a 50-m pile depth. The maximum dimensionless soil temperature is 0.77, and the minimum value is 0.07 of piles with 30 m depth in Figure 7b.
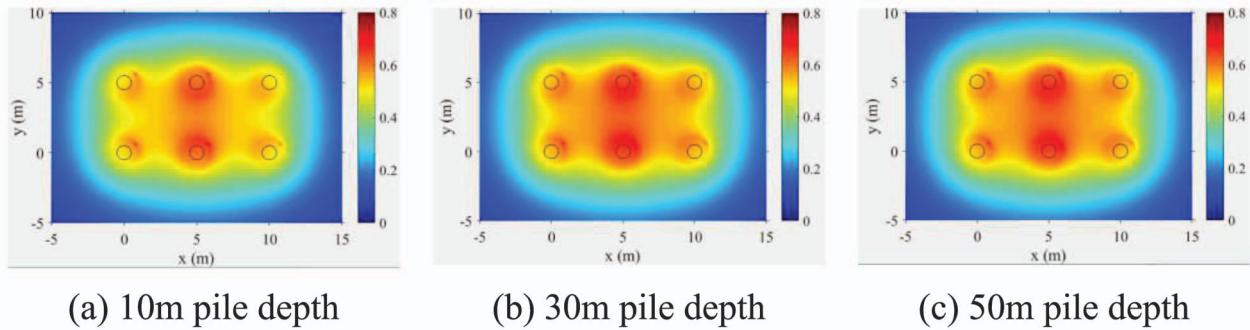
(a) 10m pile depth   (b) 30m pile depth   (c) 50m pile depth

Figure 7. *Dimensionless soil temperature distribution influenced by different pile depths (v = 0, pile layout = 3 × 2, pile spacing distance = 5 m).*

(a) Different groundwater velocities

(b) Different pile layouts

(c) Different pile spacing distances
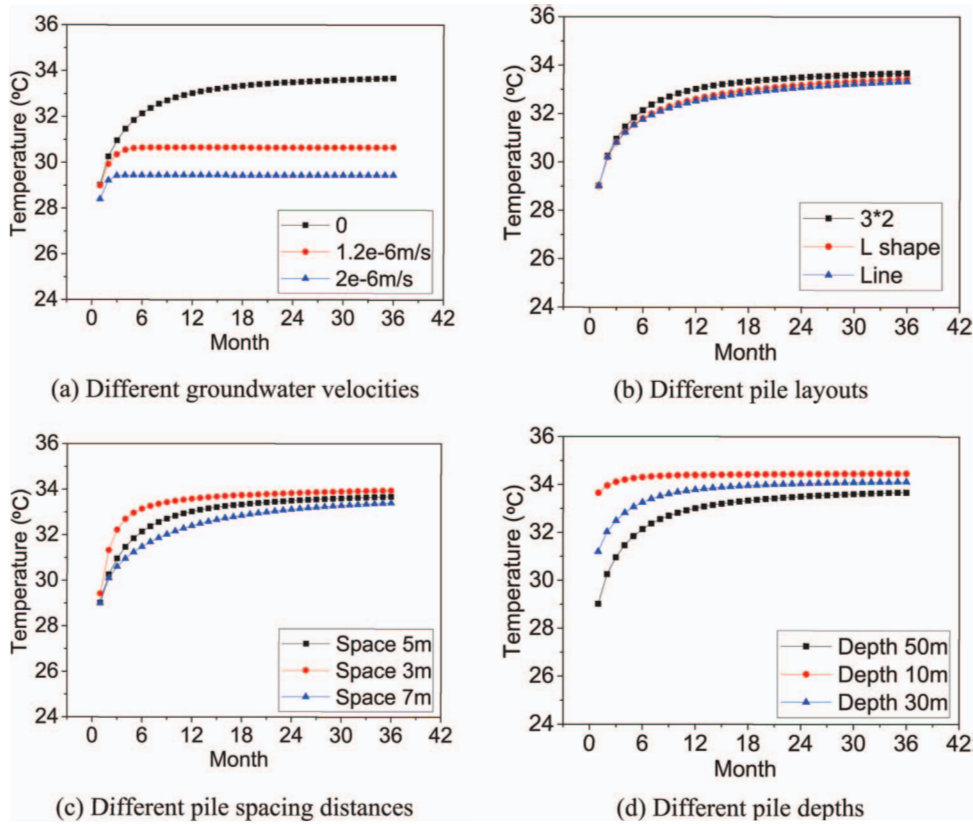
(d) Different pile depths

Figure 8. *Average outlet temperature of energy piles influenced by different factors (inlet fluid temperature and velocity of energy piles are 35°C and 0.8 m/s).*

Taking the energy pile group with the 3 × 2 layout, no groundwater, 5 m pile spacing and 50 m pile depth as the baseline, the typical dimensionless soil temperatures of the energy pile groups with different factors are compared and summarized in Table 2.

When the groundwater velocity increases from 0 to 1.2 × 10^{-6} m/s and 2.0 × 10^{-6} m/s, the maximum dimensionless soil temperature decreases from 0.77 to 0.61 and 0.45. When the pile layout is changed from 3 × 2 to L shape and line shape, the maximum dimensionless soil temperature decreases from 0.77 to 0.65 and 0.61. When the 5-m pile spacing distance decreases to 3 m and increases to 7 m, the maximum dimensionless soil temperature increases from 0.77 to 1.13 and decreases to 0.59.

As for the pile depth in the range of 10~50 m, their typical dimensionless soil temperatures are quite similar due to the small thermal influence of soil surface.

3.2. Outlet fluid temperatures under different conditions of inlet fluid

The outlet fluid temperature of energy piles varies for piles with different groundwater velocities, pile layouts, pile spacing distances and pile depths. For different inlet fluid temperatures and velocities, the influential levels of the above factors are different.

Table 2. *Typical dimensionless soil temperatures of different energy pile groups.*

	Baseline	Groundwater velocity		Layout		Pile spacing distance		Pile depth	
	Layout: 3 × 2, v: 0 m/s, spacing: 5 m, depth: 50 m	1.2×10^{-6} m/s	2.0×10^{-6} m/s L	Line		3 m	7 m	10 m	30 m
Minimum	0.07	0	0	0.01	0.06	0.26	0.02	0.06	0.07
Maximum	0.77	0.61	0.45	0.65	0.61	1.13	0.59	0.75	0.77
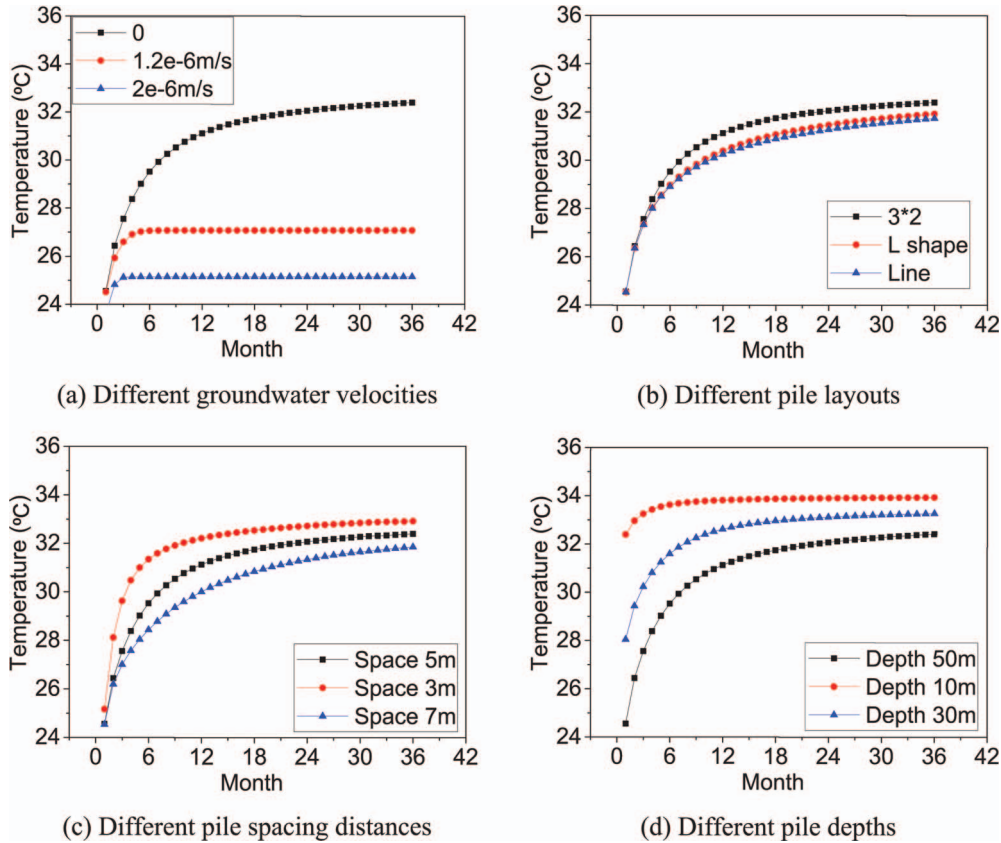
Figure 9. *Average outlet temperature of energy piles influenced by different factors (inlet fluid temperature and velocity of energy piles are 35°C and 0.4 m/s).*

(a) Different groundwater velocities
(b) Different pile layouts
(c) Different pile spacing distances
(d) Different pile depths

Figure 8 shows the outlet fluid temperature of energy piles influenced by different factors when the inlet fluid temperature and velocity of energy piles are 35°C and 0.8 m/s. In Figure 8a, when the groundwater velocity increases from 0 to 1.2×10^{-6} m/s and 2.0×10^{-6} m/s, the outlet fluid temperature decreases from 33.7 to 30.6°C and 29.4°C after a 3-year operation. The high groundwater velocity is of benefit to the low outlet fluid temperature of piles because the heat released by the piles can be easily taken away by the groundwater. Even so, the increase in groundwater velocity contributes less to the decrease in outlet fluid temperature when the groundwater velocity becomes larger.

Figure 8b reflects that the pile layout has a small influence on the outlet fluid temperature because the pile number is small. Despite the relatively compact 3 × 2 layout, each pile is in the boundary of the pile group and the heat can disperse easily to the surrounding soil. As for the piles in line layout, the thermal interaction between piles is the smallest. The outlet fluid temperature of piles in 3 × 2 layout, L layout and line layout is respectively 33.0, 32.6 and 32.5°C after the 1-year operation, and 33.7, 33.4 and 33.3°C after the 3-year operation.

It is obvious in Figure 8c when the pile spacing distance increases from 3 to 5 and 7 m, the increasing rate of outlet fluid temperature becomes lower; the values of outlet fluid temperatures in these three cases become closer as the time becomes longer. It means that at the primary stage the influence of pile spacing is large because the thermal dispersing radius of piles is less than 7 m pile spacing distance. The outlet fluid temperatures of the pile with spacing distance at 3, 5 and 7 m are respectively 33.6, 33.0 and 29.4°C after the 1-year operation, and 33.9, 33.7 and 33.4°C after the 3-year operation.
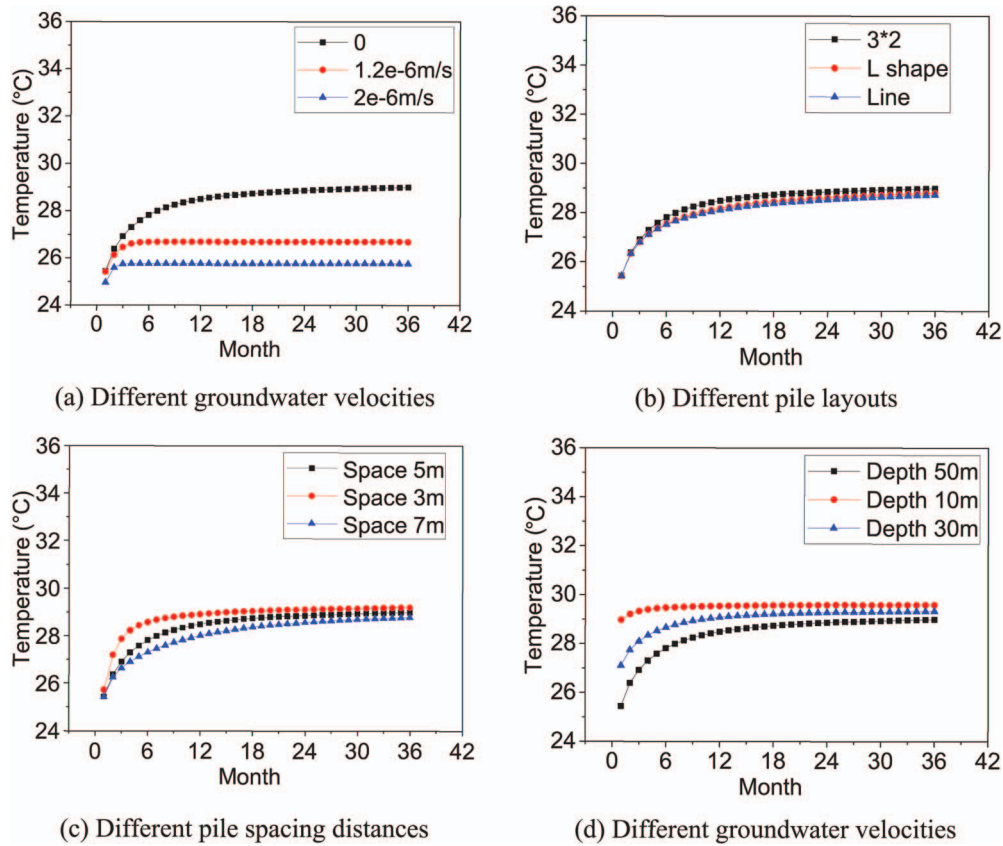
Figure 10. *Average outlet temperature of energy piles influenced by different factors (inlet fluid temperature and velocity of energy piles are 30°C and 0.8 m/s).*

Figure 8d shows the influences of pile depth on the outlet fluid temperature. The increasing depth contributes to the fast increase in the outlet fluid temperature at the primary stage because the percentage of heat dispersed from the soil surface is small in the long piles. As time becomes longer, this contribution becomes smaller and the temperatures of piles with different depths tend to closer. The outlet fluid temperatures of piles with 10, 30 and 50 m are respectively 34.4, 33.8 and 33.0°C after the 1-year operation, and 34.5, 34.1 and 33.7°C after the 3-year operation.

When the fluid velocity of energy piles reduces from 0.8 to 0.4 m/s, the influential factors on the outlet temperature of piles are shown in Figure 9. Compared to Figure 8, Figure 9 shows that the decrease in fluid velocity enlarges the influential levels of different factors because the heat transfer takes a longer time to reach a relatively steady status.

In Figure 9a, when the groundwater velocity increases from 0 to 1.2 × 10⁻⁶ m/s and 2.0 × 10⁻⁶ m/s, the outlet fluid temperature decreases from 32.4 to 27.1 and 25.1°C after the 3-year operation. Figure 9b shows that the outlet fluid temperature of the pile in 3 × 2 layout, L layout and line layout is respectively 31.1, 30.4 and 30.2°C after 1-year operation, and 32.4, 31.9 and 31.7°C after the 3-year operation. Figure 9c reflects that the outlet fluid temperature of the pile with spacing distance at 3, 5 and 7 m is respectively 32.2, 31.1 and 30.0°C after the 1-year operation, and 32.9, 32.4 and 31.9°C after the 3-year operation. In Figure 9d,
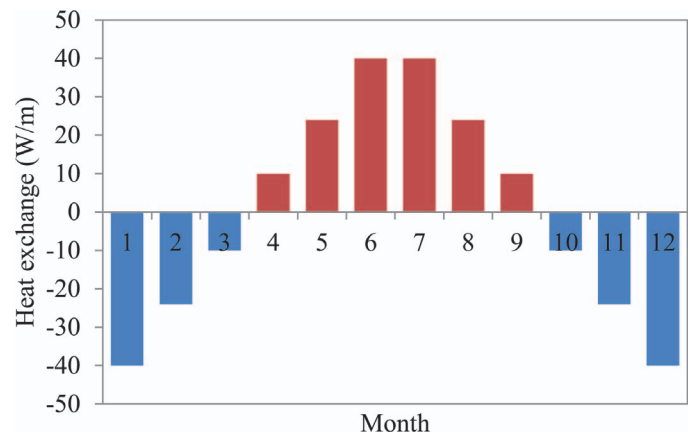

Figure 11. *Monthly soil heat exchange of energy pile group.*

the outlet fluid temperatures of the pile with 10, 30 and 50 m is respectively 33.8, 32.6 and 31.1°C after the 1-year operation, and 33.9, 33.3 and 32.4°C after the 3-year operation.

Even though reducing the fluid temperature or velocity of energy piles both can reduce the released heat of energy piles at the primary stage, the influential level of different factors on the outlet fluid temperature is different under these two different cases. Figure 10 shows that when the inlet fluid temperature of
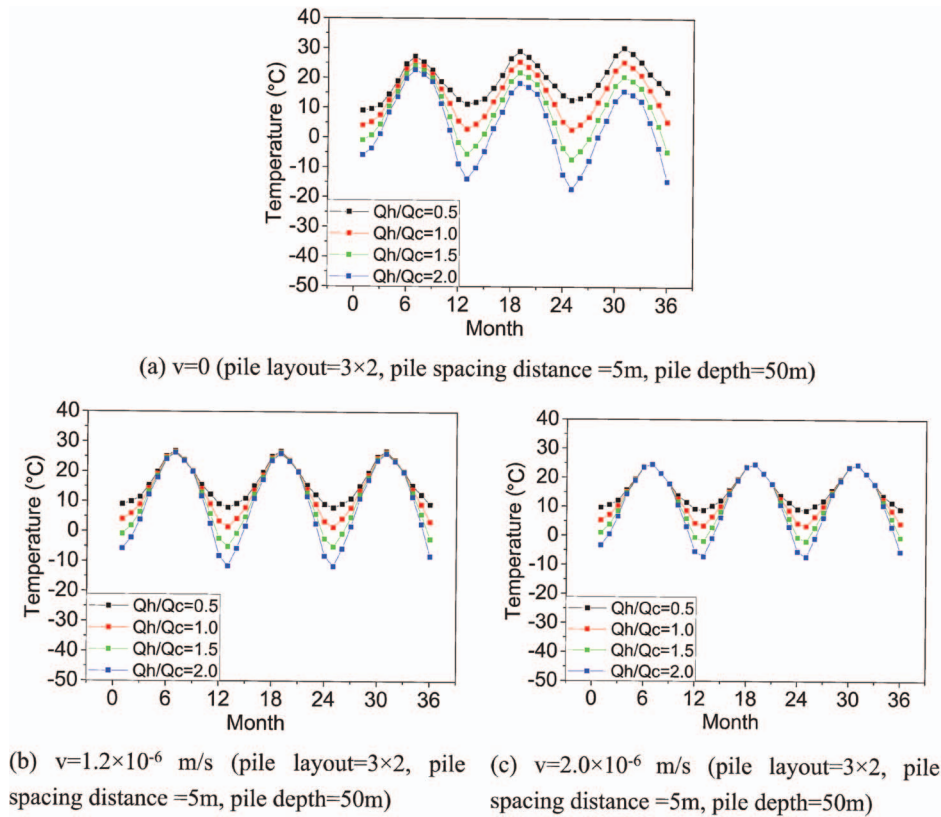
Figure 12. *Outlet temperatures of energy piles influenced by different groundwater velocities.*

energy piles reduces from 35 to 30°C, the influential factors on the outlet temperature of piles are shown in Figure 10. Comparing Figure 10 to Figure 8, the decrease in the inlet fluid temperature reduces the influential levels of different factors because the heat transfer takes a shorter time to reach a relatively steady status.

In Figure 10a, when the groundwater velocity increases from 0 to 1.2×10^{-6} m/s and 2.0×10^{-6} m/s, the outlet fluid temperature decreases from 29.0 to 26.7 and 25.8°C after the 3-year operation. Figure 10b shows that the outlet fluid temperature of the pile in 3×2 layout, L layout, and line layout is respectively 28.5, 28.2 and 28.1°C after the 1-year operation, and 29.0, 28.8 and 28.7°C after the 3-year operation. Figure 10c reflects that the outlet fluid temperature of the pile with spacing distance at 3, 5 and 7 m is respectively 28.9, 28.5 and 28.0°C after the 1-year operation, and 29.2, 29.0 and 28.8°C after the 3-year operation. In Figure 10d, the outlet fluid temperature of the pile with 10, 30 and 50 m is respectively 29.5, 29.5 and 28.5°C after the 1-year operation, and 29.6, 29.6 and 29.0°C after the 3-year operation.

The comparison among Figures 8–10 shows that the decrease in inlet fluid velocity (Figures 8 and 9) makes the different factors (groundwater velocity, pile layout, pile spacing distance and pile depth) have more obvious influential levels on thermal performance of energy piles than the decrease in inlet fluid temperature (Figures 8 and 10). When the inlet fluid velocity decreases from 0.8 to 0.4 m/s, the temperature decrease in outlet fluid temper-

ature changes from 12.59 to 22.39% caused by the increase in groundwater velocity from 0 to 2.0×10^{-6} m/s, changes from 1.04 to 2.03% caused by the change of pile layout from 3×2 to line shape, changes from 1.61 to 3.23% caused by the increase in pile spacing distance from 3 to 7 m and changes from 2.32 to 4.69% caused by the increase in pile depth from 10 to 50 m. When the inlet fluid temperature decreases from 35 to 30°C, the temperature decrease in outlet fluid temperature changes from 12.59 to 11.14% caused by the increase in groundwater velocity from 0 to 2.0×10^{-6} m/s, changes from 1.04 to 0.92% caused by the change of pile layout from 3×2 to line shape, changes from 1.61 to 1.43% caused by the increase in pile spacing distance from 3 to 7 m, changes from 2.32 to 2.05% caused by the increase in pile depth from 10 to 50 m.

3.3. Outlet fluid temperature influenced by different heat exchange ratios

For energy piles in different GSHP systems, the monthly soil heat exchange usually varies relying on the different heating and cooling demands of buildings. Figure 11 shows the monthly heat extraction and injection rates of the energy pile group during heating and cooling seasons. For piles with different depths, the inputted specific heat flux rate (i.e. heat flux rate per depth) of an energy pile is the same and the total heat flux of each energy pile is different. This is because in practical application, the energy
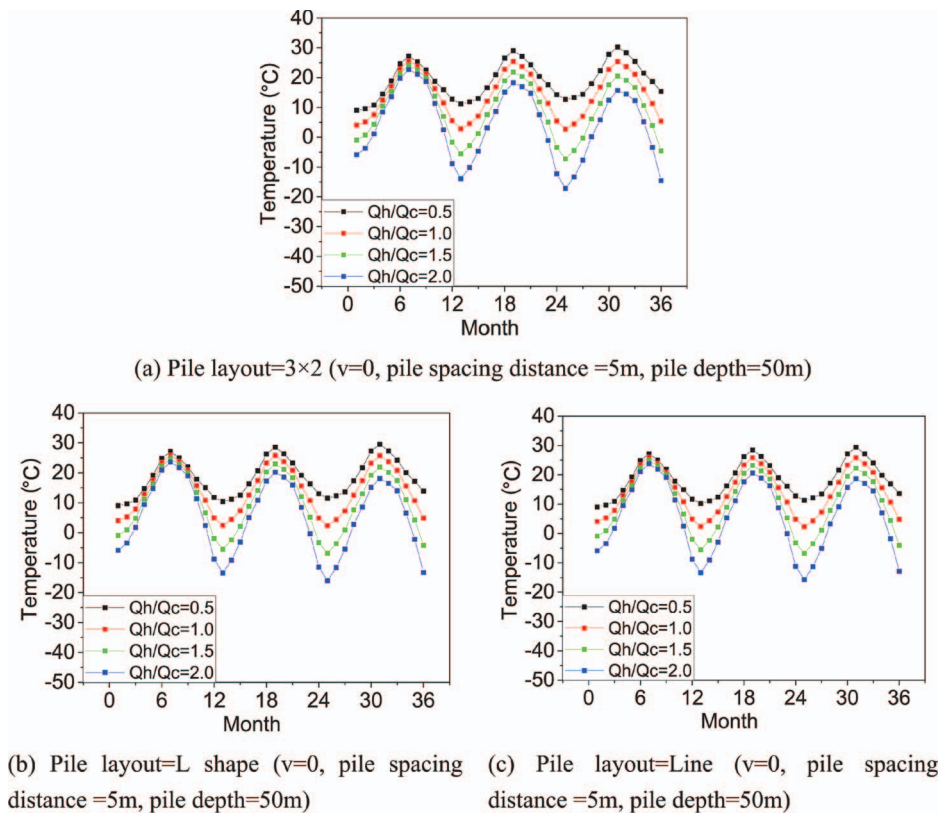
(a) Pile layout=3×2 (v=0, pile spacing distance =5m, pile depth=50m)

(b) Pile layout=L shape (v=0, pile spacing distance =5m, pile depth=50m)

(c) Pile layout=Line (v=0, pile spacing distance =5m, pile depth=50m)

Figure 13. *Outlet temperatures of energy piles influenced by different pile layouts.*
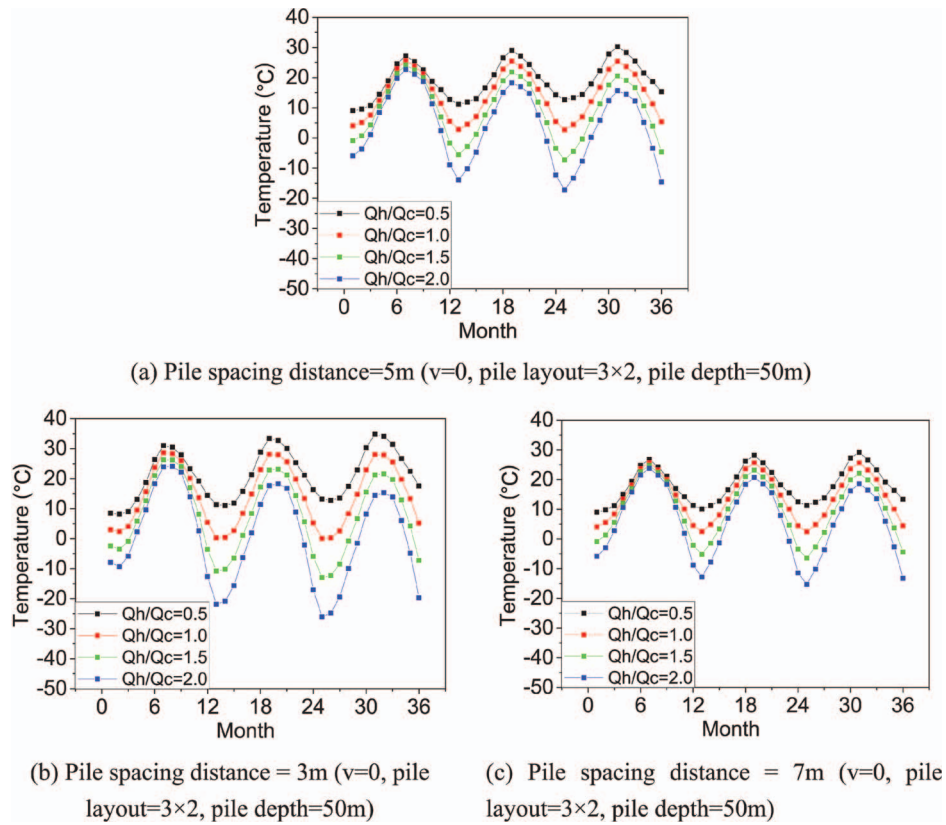
pile is usually designed or evaluated by the specific heat flux rate empirically.

In Figure 11, the ratio of heat extraction to heat injection is 1, which means the annual soil thermal exchange is balanced. However, in most GSHP systems, heating or cooling is dominated. Thus, in the simulation, the amount of heat extraction is adjusted by timing the indexes of 0.5, 1.5 and 2.0 and consequently the ratio of heat extraction to heat injection can be 0.5, 1.0, 1.5 and 2.0. Since the total soil heat exchange of the energy pile group is known in cases of this section, the inlet temperature, outlet temperature and heat flux of each energy pile can be calculated iteratively. With different heat exchange ratios of energy piles, the influential levels of different factors on the outlet fluid temperatures of piles in three operation years are investigated as shown in Figures 12–15.

The influence of groundwater velocities on outlet fluid temperature in three operation years is shown in Figure 12 with different heat exchange ratios. When the groundwater velocity is larger than 1.2×10^{-6} m/s, the annually average outlet fluid temperature variation caused by the different heat exchange ratios is not obvious and the temperature variations are nearly the same in summer because the soil thermal transfer is large and the soil temperature can be easily recovered to the initial value when the groundwater velocity is large. No matter what the value of soil heat extraction is, the soil can recover to a similar temperature at the beginning of summer. When groundwater velocity is 0, the maximum outlet fluid temperature is 30.3, 25.7, 24.2 and 22.7°C,

and the minimum outlet fluid temperature is 9.0, 2.7, −7.2 and −17.2°C with the heat exchange ratios of 0.5, 1.0, 1.5 and 2.0. When groundwater velocity is 1.2×10^{-6} m/s, the maximum outlet fluid temperature is 26.8, 26.6, 26.4 and 26.2°C, and the minimum outlet fluid temperature is 8.0, 1.4, −5.1 and −11.6°C with the heat exchange ratios of 0.5, 1.0, 1.5 and 2.0. When groundwater velocity is 2.0×10^{-6} m/s, the maximum outlet fluid temperature is 24.6, 24.6, 24.6 and 24.6°C, and the minimum outlet fluid temperature is 8.7, 3.4, −1.9 and −7.2°C with the heat exchange ratios of 0.5, 1.0, 1.5 and 2.0. Results show that the small groundwater velocity enlarges the variation of outlet fluid temperature influenced by different heat exchange ratios.

The influence of the pile layout on outlet fluid temperature in three operation years is shown in Figure 13 with different heat exchange ratios. When the pile layout changes from 3×2 to line shape, the influence of different heat exchange ratios on the outlet fluid temperature variation becomes small. When the pile layout is 3×2, the maximum outlet fluid temperature is 30.3, 25.7, 24.2 and 22.7°C, and the minimum outlet fluid temperature is 9.0, 2.7, −7.2 and −17.2°C with the heat exchange ratios of 0.5, 1.0, 1.5 and 2.0. When pile layout is L shape, the maximum outlet fluid temperature is 29.5, 26.0, 24.8 and 23.6°C, and the minimum outlet fluid temperature is 9.0, 2.3, −6.8 and −16.0°C with the heat exchange ratios of 0.5, 1.0, 1.5 and 2.0. When pile layout is line shape, the maximum outlet fluid temperature is 29.4, 26.0, 24.9 and 23.8°C, and the minimum outlet fluid temperature is 9.0,

(a) Pile spacing distance=5m (v=0, pile layout=3×2, pile depth=50m)

(b) Pile spacing distance = 3m (v=0, pile layout=3×2, pile depth=50m)

(c) Pile spacing distance = 7m (v=0, pile layout=3×2, pile depth=50m)

Figure 14. *Outlet temperatures of energy piles influenced by different pile spacings.*

2.3, −6.7 and −15.8°C with the heat exchange ratios of 0.5, 1.0, 1.5 and 2.0.

The influence of the pile spacing distance on outlet fluid temperature in three operation years is shown in Figure 14 with different heat exchange ratios. The heat exchange ratios of 1.5 and 2.0 cause the decrease in outlet fluid temperature, the heat exchange ratio of 1.0 keeps the outlet fluid temperature steady and the heat exchange ratio of 0.5 causes the increase in outlet fluid temperature. When pile spacing distance is 5 m, the maximum outlet fluid temperature is 30.3, 25.7, 24.2 and 22.7°C, and the minimum outlet fluid temperature is 9.0, 2.7, −7.2 and −17.2°C with the heat exchange ratios of 0.5, 1.0, 1.5 and 2.0. When pile spacing distance is 3 m, the maximum outlet fluid temperature is 34.8, 28.7, 26.3 and 24.1°C, and the minimum outlet fluid temperature is 8.2, 0.5, −13.0 and −26.1°C with the heat exchange ratios of 0.5, 1.0, 1.5 and 2.0. When pile spacing distance is 7 m, the maximum outlet fluid temperature is 29.2, 25.8, 24.8 and 23.8°C, and the minimum outlet fluid temperature is 9.0, 2.4, −6.4 and −15.3°C with the heat exchange ratios of 0.5, 1.0, 1.5 and 2.0. Results show that the small pile spacing distance enlarges the variation of outlet fluid temperature influenced by different heat exchange ratios.

With different heat exchange ratios, the influence of the pile depth on outlet fluid temperature in three operation years is shown in Figure 15. When the pile depth changes from 10 to 50 m, the influence of different heat exchange ratios on the outlet fluid

temperature variation becomes large. The piles with 10-m depth have a strong ability of heat recovery because the unbalanced heat can be supplemented from the ground surface. When pile depth is 10 m, the maximum outlet fluid temperature is 29.8, 28.0, 27.0 and 26.0°C, and the minimum outlet fluid temperature is 8.2, 0.5, −8.4 and −17.3°C with the heat exchange ratios of 0.5, 1.0, 1.5 and 2.0. When pile depth is 30 m, the maximum outlet fluid temperature is 30.9, 26.5, 25.0 and 23.5°C, and the minimum outlet fluid temperature is 8.6, 1.9, −8.3 and −18.5°C with the heat exchange ratios of 0.5, 1.0, 1.5 and 2.0. When pile depth is 50 m, the maximum outlet fluid temperature is 30.3, 25.7, 24.2 and 22.7°C, and the minimum outlet fluid temperature is 9.0, 2.7, −7.2 and −17.2°C with the heat exchange ratios of 0.5, 1.0, 1.5 and 2.0.

4. CONCLUSIONS

A three-dimensional analytical model of the spiral coil energy pile group with seepage is used to analyze the influence of the geometrical parameters (the pile depth, pile spacing and pile layout) and external parameter (the groundwater velocity) on the heat transfer of pile groups. It considers the thermal interaction among different energy piles, the geometry of the spiral pipe and the velocity of groundwater. Major conclusions are as follows:
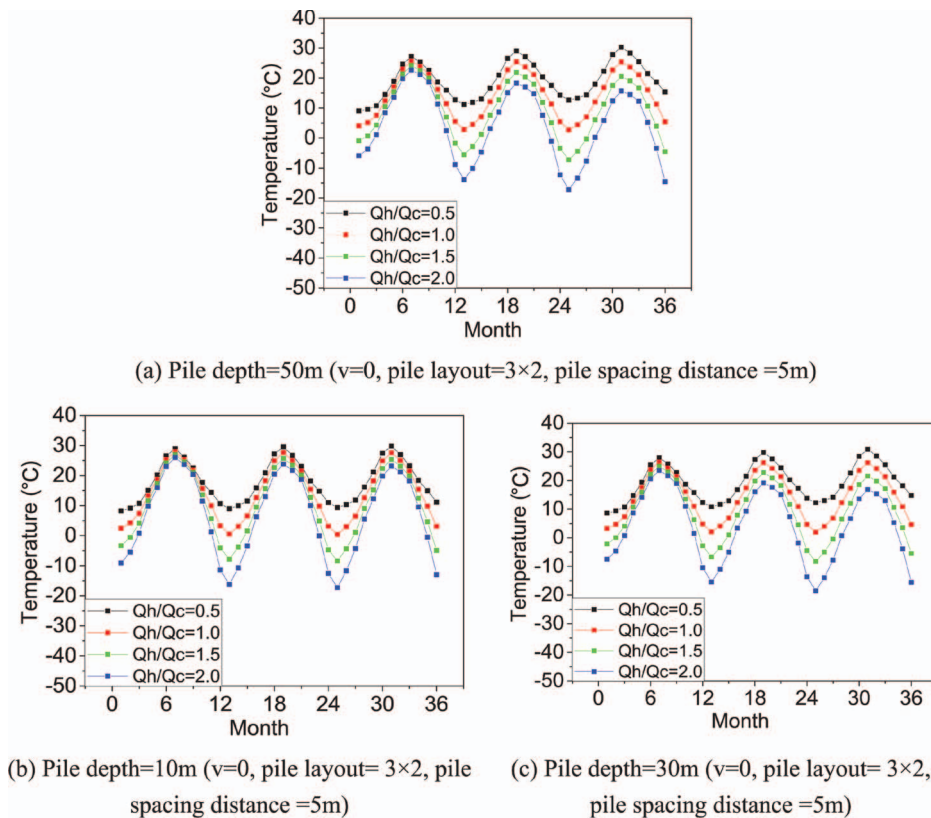
(a) Pile depth=50m (v=0, pile layout=3×2, pile spacing distance =5m)

(b) Pile depth=10m (v=0, pile layout= 3×2, pile spacing distance =5m)

(c) Pile depth=30m (v=0, pile layout= 3×2, pile spacing distance =5m)

Figure 15. *Outlet temperatures of energy piles influenced by different pile depths.*

(1) Groundwater flow and other parameters play important roles in affecting the heat and mass transfer of energy pile groups. The maximum dimensionless soil temperature decreases from 0.77 to 0.61 and 0.45, from 0.77 to 0.65 and 0.61, from 1.13 to 0.77 and 0.59 and from 0.77 to 0.77 and 0.75, respectively; when groundwater velocity increases from 0 to 1.2×10^{-6} and 2.0×10^{-6} m/s, the energy pile layout changes from 3×2 to L shape and line shape, the pile spacing distance increases from 3 to 7 m and the pile depth decreases from 50 to 10 m. The contribution of the groundwater velocity increases to keeping steady soil temperature is the most obvious among different factors.

(2) When the fluid velocity inside the pipe is low, the influence of groundwater velocity, pile layout, pile spacing distance and pile depth on the outlet fluid temperature is more obvious. Taking the pile layout as an example, when the inside fluid velocity decreases from 0.8 to 0.4 m/s, the temperature decrease of the outlet fluid temperature changes from 1.04 to 2.03% caused by the change of pile layout from 3×2 to line shape.

(3) The large groundwater velocity, line shape pile layout, large pile spacing distance and short pile depth can alleviate the long-term temperature variation caused by the unbalanced soil heat exchange. Taking the $Q_h/Q_c = 0.5$ as an example, when the pile layout changes from 3×2 to line shape, the maximum outlet fluid temperature decreases from 30.3 to 29.4 °C after a 3-year operation.

This research work on investigating the influential factors of the energy pile group will facilitate the research, design and application of the energy pile groups in ground source heat pumps.

ACKNOWLEDGEMENTS

REFERENCES

[1] Gan G. Dynamic thermal modelling of horizontal ground-source heat pumps. *Int J Low-Carbon Tech* 2013;**8**(2):95–105.

[2] Wu Y, Gan G, Gonzalez R, *et al.* Prediction of the thermal performance of horizontal-coupled ground-source heat exchangers. *Int J Low-Carbon Tec* 2011;**6**(4):261–269.

[3] Florides G, Kalogirou S. Ground heat exchangers—A review of systems, models and applications. *Renew Energ* 2007;**32**(15):2461–2478.

[4] Javed S, Fahlén P. Thermal response testing of a multiple borehole ground heat exchanger. *Int J Low-Carbon Tec* 2011;**6**(2):141–148.

[5] Cui Y, Zhu J, Meng F. Techno-economic evaluation of multiple energy piles for a ground-coupled heat pump system. *Energ Convers Manage* 2018;**178**:200–16.

[6] Bottarelli M. A preliminary testing of a flat panel ground heat exchanger. *Int J Low-Carbon Tec* 2013;**8**(2):80–87.

[7] Cui Y, Zhu J. Year-round performance assessment of a ground source heat pump with multiple energy piles. *Energ Build* 2018;**158**:509–24.

[8] You T, Li X, Cao S *et al.* Soil thermal imbalance of ground source heat pump systems with spiral-coil energy pile groups under seepage conditions and various influential factors. *Energ Convers Manage* 2018;**178**:123–36.

[9] Fadejev J, Simson R, Kurnitski J *et al.* A review on energy piles design, sizing and modelling. *Energy* 2017;**122**:390–407.

[10] Moon C, Choi J. Heating performance characteristics of the ground source heat pump system with energy-piles and energy-slabs. *Energy* 2015;**81**:27–32.

[11] Li X, Chen Y, Chen Z, *et al.*, Thermal performances of different types of underground heat exchangers, *Energ Build* 2006;**38**(5):543–547.

[12] Gao J, Zhang X, Liu J, *et al.*, Thermal performance and ground temperature of vertical pile-foundation heat exchangers: A case study, *Appl Therm Eng* 2008;**28**(17–18):2295–2304

[13] Cui P, Li X, Man Y, *et al.* Heat transfer analysis of pile geothermal heat exchangers with spiral coils. *Appl Energ* 2011;**88**(11):4113–4119.

[14] Zhang W, Yang H, Lu L, *et al.* Investigation on heat transfer around buried coils of pile foundation heat exchangers for ground-coupled heat pump applications. *Int J Heat Mass Trans* 2012;**55**(21–22):6023–6031.

[15] Zarrella A, De Carli M, Galgaro A. Thermal performance of two types of energy foundation pile: Helical pipe and triple U-tube. *Appl Therm Eng* 2013;**61**(2):301–310.

[16] Lee C, Lam H. A simplified model of energy pile for ground-source heat pump systems. *Energy* 2013;**55**:838–45.

[17] Hu P, Zha J, Lei F *et al.* A composite cylindrical model and its application in analysis of thermal response and performance for energy pile. *Energy and buildings* 2014;**84**:324–332.

[18] Noorollahi Y, Saeidi R, Mohammadi M *et al.* The effects of ground heat exchanger parameters changes on geothermal heat pump performance–a review. *Appl Therm Eng* 2018;**129**:1645–58.

[19] Zhang W, Yang H, Lu L *et al.* Study on spiral source models revealing groundwater transfusion effects on pile foundation ground heat exchangers. *Int J Heat Mass Trans* 2015;**84**:119–29.

[20] Cimmino M, Bernier M, Adams F. A contribution towards the determination of g-functions using the finite line source. *Appl Ther Eng* 2013;**51**(1–2):401–412.

[21] Choi J, Park J, Lee S. Numerical evaluation of the effects of groundwater flow on borehole heat exchanger arrays. *Renew Energ* 2013;**52**:230–40.

[22] Zhao Q, Liu F, Liu C *et al.* Influence of spiral pitch on the thermal behaviors of energy piles with spiral-tube heat exchanger. *Appl Ther Eng* 2017;**125**:1280–90.

[23] Zhang W, Zhang L, Cui P *et al.* The influence of groundwater seepage on the performance of ground source heat pump system with energy pile. *Appl Ther Eng* 2019;**162**:114217.

[24] You S, Cheng X, Yu C *et al.* Effects of groundwater flow on the heat transfer performance of energy piles: Experimental and numerical analysis. *Energ Build* 2017;**155**:249–59.

[25] Yoon S, Lee S, Xue J *et al.* Evaluation of the thermal efficiency and a cost analysis of different types of ground heat exchangers in energy piles. *Energ Convers Manag* 2015;**105**:393–402.

[26] Zhao Q, Chen B, Liu F. Study on the thermal performance of several types of energy pile ground heat exchangers: U-shaped W-shaped and spiral-shaped. *Energ Build* 2016;**133**:335–44.

[27] Yang W, Lu P, Chen Y. Laboratory investigations of the thermal performance of an energy pile with spiral coil ground heat exchanger. *Energ Build* 2016;**128**:491–502.

[28] Carslaw H, Jeager J. 1959. *Conduction of Heat in Solids* 2nd edn. Oxford: Oxford Press.